

## **Preliminary Investigation of Generation of Guerilla-Heavy Rainfall Using Himawari-8 and XRAIN Information in Kinki Region**

Wendi HARJUPA<sup>(1)</sup>, Eiichi NAKAKITA, Yasuhiko SUMIDA<sup>(2)</sup>  
and Kosei YAMAGUCHI

(1) Graduate School of Engineering, Kyoto University

(2) Meteorological Satellite Center, JMA

### **Synopsis**

The preliminary study of utilization of Himawari-8 observation data and XRAIN data to investigate the generation of Guerilla-heavy rainfall (GHR) in Kinki region will be described in this paper. The image of cloud captured by Himawari-8 observation appear displaced because of the parallax effect in its observation. 16 pairs of brightness temperature (BT; band13) of Himawari-8 observational data overlaid with radar observational data to retrieve the linear equation to solve parallax effect. The linear equation finally will relocate the displaced of cloud image to the original location. The correctness of relocated cloud will be confirmed by comparing the estimated cloud top height and precipitation top height. The movement vector of BT was applied to solve parallax effect for band 03 visible channel. The RDCA index which developed by calculation of some observation bands data of Himawari-8 is used to predict the occurrence of radar echo aloft which can cause GHR. The RDCA identification location then next is corrected by movement vector of BT in parallax correction of visible band (03). By some cases which have been analyzed we propose the using of RDCA to predict the occurrence of GHR.

**Keywords:** RDCA, GHR, baby rain cell, Himawari-8, XRAIN, parallax

### **1. Introduction**

Localized heavy rainfall is one of the triggering factors for flash floods in or landslides around urban area. In Japan, localized torrential rainfall generated by an isolated rapidly-growing cumulonimbus cloud is

called "Guerilla-heavy rainfall" (GHR for abbreviation). In 2008, within 30 minutes an isolated cumulonimbus cloud developed around Osaka-Bay Area and brought a downpour to cause a flash flood in

Toga River in Kobe. As the flood came so rapidly without any time for response, this disaster caused five people dead. Therefore, for securing more time for warning alert before flood occurrence, it is very important to investigate the initiation mechanism of GHR and to develop a method to predict its occurrence. For early detection of a GHR, Nakakita et al. (2010) discovered that the first radar echo aloft called as “baby rain cell” inside a single cumulonimbus cloud is an important signal in the initiation stage. Then, to identify a baby rain cell of GHR, a methodology has been proposed by analyzing the vertical vorticity, greater than or equal to  $0.03\text{s}^{-1}$ , in the observation data of the extended radar information network (XRAIN) operated by Ministry of Land, Infrastructure, Transport and Tourism (MLIT). According to case studies, this methodology can detect baby rain cells aloft by 23.6 minutes on average before corresponding rainfalls were recorded by rain gauges on the ground. This methodology has been implemented in the XRAIN for real-time early warning practice (Nakakita et al., 2017; references therein).

To save more time much earlier before a GHR occurrence is very critical for safe evacuation of people during a heavy rainfall event. In this study we would like to utilize Himawari-8 observation data with XRAIN data for analysis. This study focused on the signal in the growth stage of cumulonimbus cloud development before the occurrence of baby rain cell. The development of cumulonimbus cloud is divided into three stages, growth (cumulus), mature and dissipation stage (Chilsom, A. J. and Renick, J. H., 1972). As the Himawari-8 data has fine temporal and spatial resolutions (2.5 minutes, 0.5-2 km) (Bessho et al., 2015), it can provide very valuable information for finding the important feature of cumulus cloud stage before the occurrence of GHR. Here we propose a new method to fix parallax effect in Himawari-8 observation. To fix parallax effect in Himawari-8

observation is important since this research focused on the small scale of cloud feature. After resolved the Himawari-8 imagery, then we use the resolved cloud to predict the first occurrence of precipitation aloft which can be captured by XRAIN. In final we proposed the Rapid Development Cumulus Area (RDCA) index which employed the relocated Himawari-8 data to predict the occurrence of baby rain cell of GHR.

## 2. Data and Methodology

The data from Himawari-8 satellite and XRAIN observation are used for this study. Himawari-8 is a Geostationary Meteorological Satellite which was launched by the Japan Meteorological Agency in 2014, and has entered operational service since July in 2015. Its operational geostationary orbit is located at about 36,000 km above the equator and  $140^\circ$  east in the space. To capture images, there are 16 observation bands, including three visible bands, three near-infrared bands, and ten infrared bands. The spatial and temporal resolution are 0.5-2 km and 2.5 minutes, respectively (Bessho et al, 2015). To investigate cloud albedo and cloud-top temperature, we used the data of visible image and brightness temperature (BT) from Bands 03 and 13, respectively. To correlate with Himawari-8 data, we also used observation data of radar echo from XRAIN. The spatial and temporal resolutions of XRAIN are 150 m in the maximum range of 80 km and 1 minute, respectively. The target area for analysis is Kinki region. By using observation data in Kinki region, we overlaid the Himawari-8 observation data with radar echo of XRAIN to find the correlation among parameters, cloud development, and corresponding rainfall. Before finding out the correlation, we first eliminated the parallax in the Himawari-8 data, as mentioned in the following section.

## 2.1 Parallax correction

The Himawari-8 satellite is located above the equator at the fixed position (140.7° E), and Japan is located 36.2048° N, 138.25.29° E. The view direction of Himawari-8 to Japan is north-west. Because the distance from Himawari-8 to sea level is not much larger than the cloud height, it exists parallax in the observation data due to variable cloud height. Comparing with rain echo from XRAIN, Figure 1 shows the location of a cloud over Japan is further north-west from its real position.

To eliminate parallax in Himawari-8 data, we used rain echoes from XRAIN as the real position of a cloud under the assumption that the rain just happened below the cloud. Then, the distance between the cloud and radar echoes is measured from the centers of cloud and radar echoes.

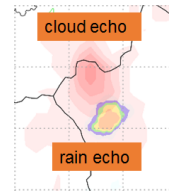


Fig. 1 Illustrative example of parallax between cloud image and radar echoes.

Figure 2 shows the samples of the distance between Himawari-8 BT image and the radar echo with parallax from Himawari-8 observation. The lowest value of BT in the cloud echo was chosen to be a starting location, and the location having a highest value of radar echo was assigned as the ending location. Since BT is correlated to the cloud height, the difference of BT caused the difference of cloud height and as the result, it will cause the difference of distance between the echoes.

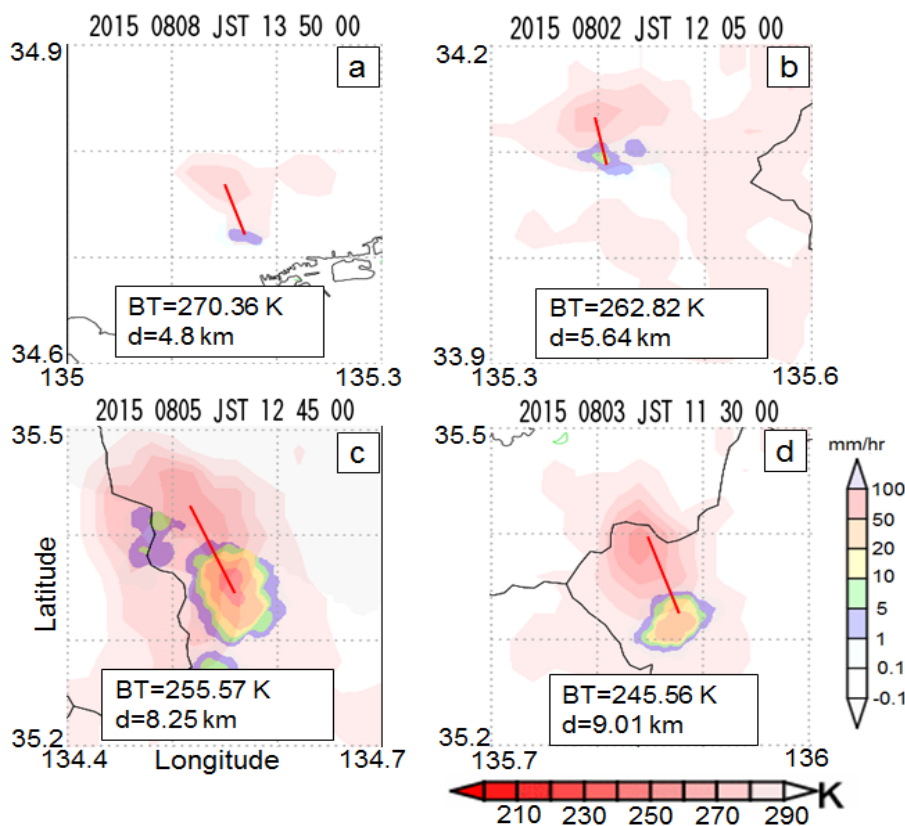


Fig. 2 Four examples of the overlay of Himawari-8 BT and radar echoes overlaid

In order to fix parallax errors in Himawari-8 data, we selected 16 events of heavy rainfall, as tabulated in Table 1. Then, with the manually-extracted 16 pairs of BT and parallax distance from the selected events, we used linear regression analysis to obtain a parallax equation, as below

$$Distance = -0.77BT + 25.5, \quad (1)$$

Where  $R^2 = 0.8744$ , the unit of distance is meter, and the unit of BT is K. The relationship between BT and parallax distances in the 16 events are shown in Figure 3.

Table 1 List of heavy rainfall event time brightness temperature.

Event	Date	Time	BT (K)
1	2015/8/1	14:20	277.52
2	2015/8/1	14:36	272.68
3	2015/8/1	14:37	264.78
4	2015/8/1	15:10	276.71
5	2015/8/1	15:14	264.60
6	2015/8/1	15:19	251.73
7	2015/8/1	15:20	244.15
8	2015/8/2	12:05	268.95
9	2015/8/3	11:20	278.51
10	2015/8/3	11:24	268.62
11	2015/8/3	11:30	245.98
12	2015/8/3	12:10	276.38
13	2015/8/3	12:15	266.37
14	2015/8/4	12:05	269.94
15	2015/8/4	13:32	266.54
16	2015/8/8	13:50	277.09

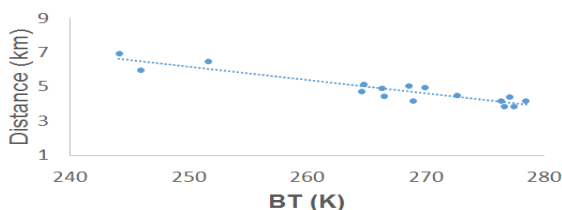


Fig. 3 Relationship between BT and parallax distance

## 2.2 Modification of Rapid Development Cumulus Area (RDCA) Index

The index of Rapid Development Cumulus Area (RDCA), developed by Meteorology Satellite Center (MSC) of Japan Meteorology Agency (JMA) (Sumida et al, 2016), is a methodology to predict the occurrence probability of thunderstorm using Himawari-8 observation data. The RDCA index is a logistic model considering the occurrence of a cumulus cloud in the basic spatial scale of 10 km<sup>2</sup> within 1 hour. The output of original RDCA is simply 0 or 1, which denotes the occurrence or non-occurrence of a thunderstorm at a targeted location within one hour, as listed in Table 2.

In this research, using the concept of RDCA index, we propose a modified RDCA index ranging from 0.1 to 0.9 for more detailed and quantitatively analyzing the occurrence probability of radar first echo aloft. The higher the modified RDCA index, the higher the probability of occurrence of rain echo. Table 2 tabulates the comparison between the indices of original RDCA and modified RDCA. For the modified RDCA index, all the parameters from Himawari-8 data are listed in table 3. There are totally 13 categories of data used for establishing the logistic model for the modified RDCA index.

Table 2 Comparison of RDCA and modified RDCA indices

Parameter	Original RDCA	Modification RDCA
Data	Himawari-8 and Lightning data	Himawari-8
Purpose	Thunderstorm detection	Radar first echo detection
Index	'0' or '1' 0= no thunderstorm 1= thunderstorm	0.1 – 0.9
Spatial resolution	0.1 x 0.1 deg	0.01 x 0.01 deg

Table 3 Parameters for modified RDCA index

No.	Detection Parameter	Main Objective
1	B03(reflectivity):Max-Ave	Detection of cloud top roughness (Day time only)
2	B03(reflectivity):Standard Deviation	
3	B13(BT):Min-Ave	Detection of cloud top roughness
4	B13(BT):Standard Deviation	
5	B16(BT) Average-B13(BT) Average	Detection of ice cloud
6	B15(BT) Average-B13(BT) Average	
7	B11(BT) Average-B13(BT) Average	
8	B08(BT) Average-B13(BT) Average	Water vapor detection above cloud top
9	B10(BT) Average-B08(BT) Average	
10	Temporal Variation of B03 (Reflectivity (average))	Presumption of developing level of cloud (Day time only)
11	Temporal Variation of B13 (BT average)	Presumption of developing level of cloud
12	Temporal Variation of B11-B13 (BT average)	Detection of developing ice cloud
13	Temporal Variation of B15-B13 (BT average)	

### 3. Result and Discussion

#### 3.1. Parallax correction

The overlay of BT and radar echoes before and after parallax corrections are shown in Figure 4a and 4b, respectively. In Figure 4, before correction, the BT echo is located in northern part of the radar echo. With the parallax equation (1), the cloud is shifted to the location above the rain echo, as shown in Fig. 4b. Using the parallax equation (1), the cloud location in

visible images from Band 03 can also be shifted to the location above the rain echo, as are shown in Fig. 5a and 5b for the before and after parallax correction. In Fig. 5a the distribution of lower cloud albedo (0.1-0.4) is eliminated to show the pair of visible and radar echoes clearly. Also, Fig. 5b shows the overlay of albedo (0.5-1) and radar echoes. The consequence of eliminating the albedo (0.1-0.4) cause the shape of cloud after parallax is different than before parallax.

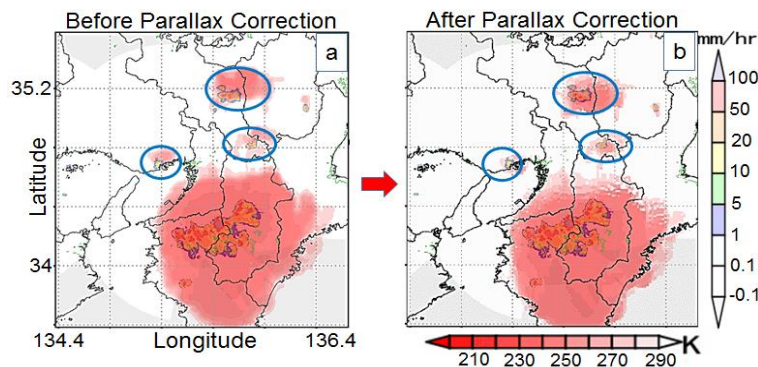


Fig. 4 Overlay of BT and radar echoes on 8 August 2015 1440 JST, a) before parallax correction, b) after parallax correction

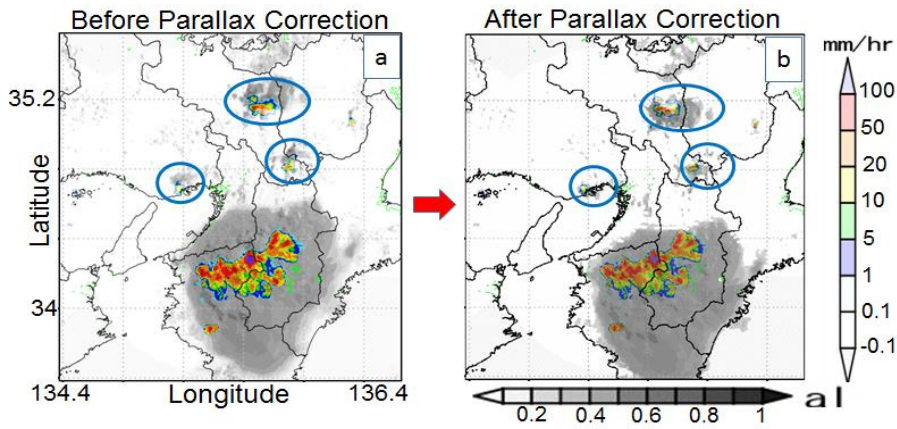


Fig. 5 Overlay of visible and radar echoes on 8 August 2015 1440 JST, a) before parallax correction, b) after parallax correction.

To verify the parallax equation, we next checked the corrected cloud height from Himawari-8 data by the height of rain observed by radars. The corrected cloud height of Himawari-8 data is already known by the BT using the parallax equation (1). Then, the information of rain height is retrieved from the three-dimensional data of radar reflectivity. Figure 6 shows the one illustrative example of comparison between the top heights of cloud and rain. At the time of 13:35, the rain top height was detected about 7,125 m by radars while the cloud top height was estimated about 9 km as the BT is 260 K. As the time evolved, at 13:45

BT decreased and the cloud top height was estimated about 10,000 m, meanwhile the rain top height detected by radars is about 9,125 meters. Finally, at 14:25 the cloud top height was estimated about 13,000 m as the BT is 230 K; the rain top height detected by radar was only 12,125 meters. Then, we performed the comparison of the estimated top heights of cloud and rain from 45 events, as shown in Fig. 7. As a result, it is obviously that the parallax equation is valid as all the estimated cloud top heights are higher than the rain top height.

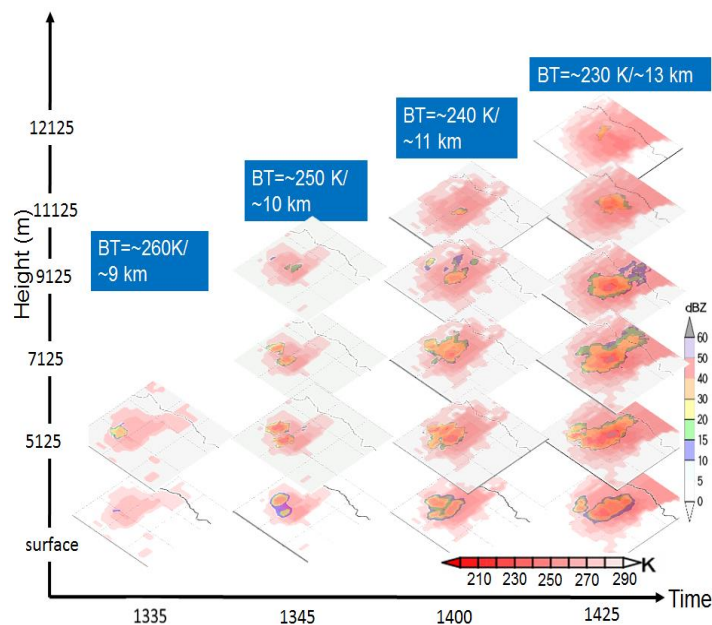


Fig. 6 One illustrative example of comparison of the estimated top heights of cloud and rain

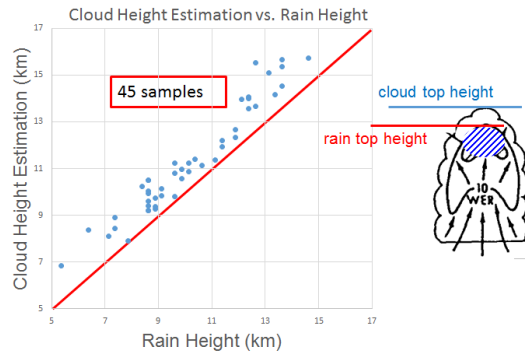


Fig. 7 Comparison results of estimated cloud top heights and rain heights from 45 events. Blue dots denote the cloud top height, and red line is the rain top height.

### 3.2 Case study of modified RDCA index

With parallax-corrected cloud data, we performed six case studies using the modified RDCA index to

verify the applicability of rain prediction, as are listed in Table 2. Particularly, we demonstrate the comparison of prediction results in the Event 1 and 2.

Table 4 Time detection differences in six events

Event	Date	Time Detection			Time difference (A-B)	Time difference (A-C)	RDCA index
		RDCA (A)	First echo aloft (B)	Rainfall on the ground (C)			
1	2015/080	13:15	13:20	13:30	5	15	0.4
2	2015/08/	13:20	13:30	13:35	10	15	0.8
3	2016/08/	13:15	13:20	13:25	5	10	0.6
4	2016/08/	11:55	12:05	12:10	10	15	0.3
5	2016/08/	13:30	13:35	13:45	5	15	0.9
6	2016/08/	13:10	13:15	13:20	5	10	0.1

#### Case 1

Figure 8 shows the results of modified RDCA index, first radar echo aloft, and rainfall recorded on the ground at different time. We discovered that the modified RDCA index first gives the value of 0.4 at 13:15, as shown in Figure 8a. Then, after five minutes, at 13:20, the first echo of rain cell was obtained from radar observation. Finally, the rainfall was detected by the rain gauges on the ground at 13:30, which is 15 minutes later than the prediction using the modified RDCA index.

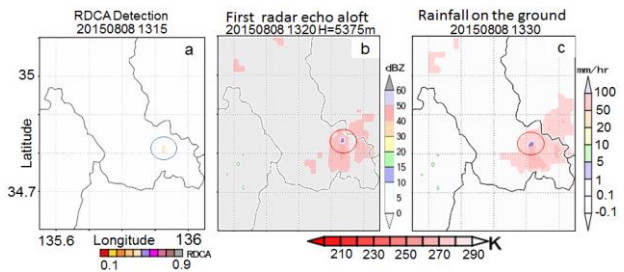


Fig. 8 Results of rain prediction using: a) modified RDCA index, b) first radar echo aloft, and c) rainfall detected on the ground.

## Case 2

Figure 9 shows the results of rain prediction in different time. In the second case, the modified RDCA index gives an index of 0.8 at 13:20. Then, after 10 minutes the first radar echo was obtained from radar observation. Finally, the rainfall was recorded on the ground at 13:35, which is also 15 minutes later than the prediction using the modified RDCA index.

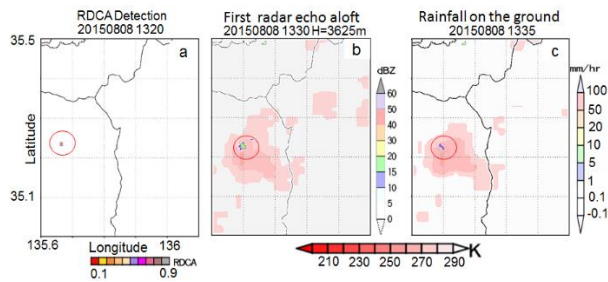


Fig. 9 Results of rain prediction using: a) RDCA index, b) first radar echo aloft, and c) rainfall detection at the ground.

## 4. Conclusions

In this preliminary study, we have investigated the capability of Himawari-8 observation data to detect the signal in the initial stage of cloud development earlier than the first radar echo aloft. To fix the parallax displacement of cloud echo in Himawari-8 we used a parallax equation obtained by using linear regression analysis with dataset of Himawari-8 BT observation and radar echoes. Then, we proposed a modified RDCA index to estimate the probability of occurrence of the first radar echo aloft. Based on several case

studies, we conclude that combining data of Himawari-8 and radar observations can predict the initial stage of a GHR before the first radar echo aloft.

## References

- Chisholm A.J., and Renick J.H. (1972): The kinematics of multicell and supercell alberta hailstorms, *Alberta Hail Studies, Alberta Research Council Report 72-2*, 24-31.
- E. Nakakita, H. Yamabe, and K. Yamaguchi. (2010): Earlier detection of the origin of very localized torrential rainfall. *Journal of Hydraulic Engineering, Japan Society of Civil Engineers*, vol. 54, pp. 343–348. (Japanese).
- E. Nakakita, H. Sato, R. Nishiwaki, H. Yamabe and K. Yamaguchi. (2017): Early detection of baby rain cell aloft in a severe storm and risk projection for urban flash flood. *Advance in Meteorology*, Article ID 5962356, 15 pages.
- K. Bessho, K. Date, M. Hayashi, A. Ikeda, T. Imai, H. Inoue, Y. Kumagai, T. Miyakawa, H. Murata, T. Ohno, A. Okuyama, R. Oyama, Y. Sasaki, Y. Shimazu, K. Shimoji, Y. Sumida. (2016): An Introduction to Himawari-8/9 - New-Generation Geostationary Meteorological Satellites, *J. Meteorol. Soc. Japan. Ser. II*, vol. 94, no. 2, pp. 151–183.
- Y. Sumida, S. Hiroshi, I. Takahito and S. Akira. (2016) *Meteorological Satellite Center Technical Note*, no. 62.

(Received June 10, 2017)